Revista Colombiana de Física, Vol. 43, No. 2 de 2011.

Phase Diagrams For Generalized Spin-1 And 3/2 Ising Model By Using Linear Chain Approximation And Monte Carlo Simulations

Diagrama De Fases Para El Modelo De Ising De Espín Generalizado $S = 1$ Y 3/2 Usando Las Técnicas De Cadena Lineal Y Simulaciones De Monte Carlo

D. Peña Lara * [a]

[a] *Departamento de Física, Universidad del Valle, A.A. 25360, Cali, Colombia.*

Recibido 30.03.10; Aceptado 06.12.10; Publicado en línea 04.09.11.

Resumen

Se estudió el modelo de Ising de espín general por la aproximación de la cadena lineal (CL) y las simulaciones de Monte Carlo (MC). Los diagramas de fases en el plano de la anisotropía reducida como función de la temperatura reducida que se obtuvieron, en particular para $\sigma = 1$ y $3/2$, son cualitativamente los mismos reportados por la teoría de campo medio y de la aproximación de pares. Para $\sigma = 1$ y a temperaturas bajas, hay una línea de primer orden y otra de segundo, las cuales se conectan en un punto especial denominado punto tricrítico (PTC) y para $\sigma = 3/2$, no se presenta el PTC, pero sí una línea de primer orden que separa las fases $m_1 = 3/2$ y $m_2 = 1/2$ y finaliza en un punto crítico multifásico aislado. Las simulaciones MC, realizadas sobre redes cúbicas simples, concuerdan con la CL. En suma, se demostró que el diagrama de fases para el modelo de Ising generalizado no depende del método sino que es intrínseco al modelo.

Palabras Clave: Modelo de Ising generalizado; Diagramas de fases; Simulaciones de Monte Carlo; Aproximación de la cadena lineal.

Abstract

The Generalized Spin Ising Model was studied using the Linear Chain Approximation (LC) and Monte Carlo (MC) Simulations. Phase diagrams in the reduced anisotropy plane as functions of reduced temperature obtained, for $\sigma = 1$ and $3/2$, are qualitatively the same as those of the usual mean field theory and pair approximation for the free energy. For $\sigma = 1$ and low temperatures there are one first- and one second-order lines, which are connected to a special point called tricritical point (TCP). For $\sigma = 3/2$, there is not TCP, but there exists a first-order line separating the phases $m_1 = 3/2$ and $m_2 = 1/2$ which ends at an isolated multiphase critical point. MC simulations on simple cubic lattices also confirm the general trend of the mean field like approach. In sum, it was shown that the phase diagram for the generalized Ising model does not depend on the method but is intrinsic to the model.

Keywords: Generalized spin Ising model; Phase diagrams; Monte Carlo simulations; Linear chain approximation.
PACS: 02.70.Uu; 75.10.Hk; 75.40.Mg.

1 Introduction

The Hamiltonian for a general spin Ising model may be written in the form

$$H = -J \sum_{\langle ij \rangle} \sigma_i \sigma_j + \Delta \sum_i \sigma_i^2, \qquad (1)$$

where the first sum runs over all pairs of nearest neighbors in the N lattice sites, $J > 0$ is the coupling constant, Δ is the crystal field or parameter of anisotropy and the spins σ_i have values $-s,\ -s+1,\ ...,\ s-1,\ s$. When $\sigma = 1$, the Hamiltonian (1) is called the Blume-Capel model [1, 2] to describe critical-tricritical phenomena in magnetic systems. For gen-

*diego.pena@correounivalle.edu.co

eral σ, this model has been investigated through mean field approximation [3]. It has been shown that for integer spins there exist one tricritical point and a disordered phase at low temperatures which are not present for semi-integer spins. In both cases, there are $\sigma-$dependent number n' of first-order lines emerging from a multiphase point at $T = 0$ inside the ferromagnetic region. For integer spins, one has $n' = \sigma$ lines where $n' - 1$ of them end up at independent isolated multicritical points while the other one joins the second-order transition line at the tricritical point. For semi-integer spins all the $n' = \sigma - \frac{1}{2}$ lines also terminate at independent isolated multicritical points.

2 The linear chain approximation

The thermodynamic properties of (1) can be calculated approximately by using the Bogolyubov variational principle [4]. According to this principle the best approximate free energy to the system described by H is the minimum of the left-hand side of the inequality

$$F_0 + \langle H - H_0\rangle_0 \geq F, \tag{2}$$

where $F_0 = -k_BT\ln(\mathrm{Tr}\exp(-\beta H_0))$ is the free energy associated to a trial Hamiltonian $H_0 = H_0(\gamma)$, with γ standing for the variational parameter, $\langle H - H_0\rangle_0$ is the thermal average taken over the ensemble defined by H_0, and F is the exact free energy.

In the linear chain approximation (LCA) [5] we choose as a trial Hamiltonian H_0 of parallel linear chains, namely,

$$H_0 = \sum_{\substack{\text{parallel}\\ \text{chain}}}\left(-J\sum_i \sigma_i\sigma_{i+1} + \Delta\sum_i \sigma_i^2 - \gamma\sum_i \sigma_i\right). \tag{3}$$

2.1 Case $\sigma = 1$

Assuming periodic boundary conditions, the transfer matrix is

$$T = \begin{pmatrix} \mathrm{e}^{K-D+g} & \mathrm{e}^{-\frac{1}{2}(D-g)} & \mathrm{e}^{-(K+D)} \\ \mathrm{e}^{-\frac{1}{2}(D-g)} & 1 & \mathrm{e}^{\frac{1}{2}(D+g)} \\ \mathrm{e}^{-(K+D)} & \mathrm{e}^{\frac{1}{2}(D+g)} & \mathrm{e}^{K-D-g} \end{pmatrix}, \tag{4}$$

with

$$K = \beta J, \qquad D = \beta\Delta, \qquad g = \beta\gamma. \tag{5}$$

A partial diagonalization of T is achieved through the matrix

$$U = \frac{1}{\sqrt{2}}\begin{pmatrix} 1 & 0 & 1 \\ 0 & \sqrt{2} & 0 \\ 1 & 0 & -1 \end{pmatrix}$$

leading to

$$V \equiv U^{-1}TU = \begin{pmatrix} V_{11} & V_{12} & V_{13} \\ V_{12} & V_{22} & V_{23} \\ V_{13} & V_{23} & V_{33} \end{pmatrix},$$

where

$$\begin{aligned} V_{11} &= \mathrm{e}^{-D}\left[\mathrm{e}^{-K} + \mathrm{e}^{K}\cosh(g)\right], \\ V_{12} &= \sqrt{2}\mathrm{e}^{-\frac{D}{2}}\cosh\left(\frac{g}{2}\right), \\ V_{13} &= \mathrm{e}^{K-D}\sinh(g), \\ V_{22} &= 1, \\ V_{23} &= \sqrt{2}\mathrm{e}^{-D/2}\sinh\left(\frac{g}{2}\right), \\ V_{33} &= \mathrm{e}^{-D}\left[\mathrm{e}^{K}\cosh(g) - \mathrm{e}^{-K}\right]. \end{aligned}$$

The eigenvalue equation is

$$\lambda^3 + a\lambda^2 + b\lambda + c = 0 \tag{6}$$

with

$$\begin{aligned} a &= -[1 + 2\mathrm{e}^{K-D}\cosh(g)], \\ b &= 2\mathrm{e}^{-2D}\sinh(2K) + 2^{-D}[\mathrm{e}^{K} - 1]\cosh(g), \\ c &= 2\mathrm{e}^{-2D}[\sinh(K) + \sinh(2K)]. \end{aligned}$$

The solutions of Eq. (6) are

$$\lambda_n = \frac{2}{3}\sqrt{p}\cos\left(\frac{1}{3}\cos^{-1}\left(\frac{q}{2\sqrt{p^3}}\right) + \frac{2n\pi}{3}\right) - \frac{a}{3} \tag{7}$$

with $n = 0, 1, 2$, and $p = a^2 - 3b$ and $q = 9ab - 2a^3 - 27c$.

To obtain the best approximate free energy per spin associated with H, we follow the minimization procedure of Eq. (2) mentioned above by setting $\partial F_0 + \lim_{N\to\infty}\langle H - H_0\rangle_0)/\partial g = 0$, where

$$\begin{aligned} F_0 &= -\lim_{N\to\infty}\frac{k_BT}{N}\ln(\mathrm{Tr}\,T^N) \\ &= -k_BT\ln\left(\frac{2}{3}\sqrt{p}\cos(\theta_n) - \frac{a}{3}\right). \end{aligned} \tag{8}$$

Here, θ_n denotes the value of $\cos^{-1}(q/2\sqrt{p^3})/3 + 2n\pi/3$ corresponding to the largest eigenvalue, λ_n. This leads to the result

$$g = (z-2)Km \tag{9}$$

with $m = -\partial F_0/\partial g$. It is not difficult to realize that the largest eigenvalue is

$$\lambda_n(K, D, g) = \lambda_0.$$

2.2 Case $\sigma = \frac{3}{2}$

The transfer matrix is

$$T = \begin{pmatrix} T_{11} & T_{12} & T_{13} & T_{14} \\ T_{12} & T_{22} & T_{23} & T_{24} \\ T_{13} & T_{32} & T_{33} & T_{34} \\ T_{14} & T_{24} & T_{34} & T_{44} \end{pmatrix}, \qquad (10)$$

where

$$\begin{aligned} T_{11} &= \mathrm{e}^{\frac{1}{4}(9K-9D+12g)}, & T_{12} &= \mathrm{e}^{\frac{1}{4}(3K-5D+4g)}, \\ T_{13} &= \mathrm{e}^{-\frac{1}{4}(3K+5D-2g)}, & T_{14} &= \mathrm{e}^{-\frac{9}{4}(K+D)}, \\ T_{22} &= \mathrm{e}^{\frac{1}{4}(K-D+2g)}, & T_{23} &= \mathrm{e}^{-\frac{1}{4}(D+g)}, \\ T_{24} &= \mathrm{e}^{-\frac{1}{4}(3K+5D+2g)}, & T_{33} &= \mathrm{e}^{\frac{1}{4}(K-D-2g)}, \\ T_{34} &= \mathrm{e}^{\frac{1}{4}(3K-5D-4g)}, & T_{44} &= \mathrm{e}^{\frac{1}{4}(9K-9D-12g)}, \end{aligned}$$

$$U = \frac{1}{\sqrt{2}} \begin{pmatrix} 0 & 1 & 1 & 0 \\ 1 & 0 & 0 & 1 \\ 1 & 0 & 0 & -1 \\ 0 & 1 & -1 & 0 \end{pmatrix}$$

and

$$U^{-1}TU \equiv V = \begin{pmatrix} V_{11} & V_{12} & V_{13} & V_{14} \\ V_{12} & V_{22} & V_{23} & V_{24} \\ V_{13} & V_{23} & V_{33} & V_{34} \\ V_{14} & V_{24} & V_{33} & V_{44} \end{pmatrix},$$

with

$$\begin{aligned} V_{11} &= \mathrm{e}^{\frac{1}{4}(K-D)}\cosh\left(\frac{g}{2}\right) + \mathrm{e}^{-\frac{1}{4}(K+g)}, \\ V_{12} &= \mathrm{e}^{-\frac{5D}{4}}\left[\mathrm{e}^{-\frac{3K}{4}}\cosh\left(\frac{g}{2}\right) + \mathrm{e}^{\frac{3K}{4}}\cosh(g)\right], \\ V_{13} &= \mathrm{e}^{-\frac{5D}{4}}\left[\mathrm{e}^{-\frac{3K}{4}}\sinh\left(\frac{g}{2}\right) + \mathrm{e}^{\frac{3K}{4}}\sinh(g)\right], \\ V_{14} &= \mathrm{e}^{\frac{1}{4}(K-D)}\sinh\left(\frac{g}{2}\right), \\ V_{22} &= \mathrm{e}^{-\frac{9D}{4}}\left[\mathrm{e}^{\frac{9K}{4}}\cosh(3g) + \mathrm{e}^{-\frac{9K}{4}}\right], \\ V_{23} &= \mathrm{e}^{\frac{9}{4}(K-D)}\sinh(3g), \\ V_{24} &= \mathrm{e}^{-\frac{5D}{4}}\left[\mathrm{e}^{\frac{3K}{4}}\sinh(g) - \mathrm{e}^{-\frac{3K}{4}}\sinh\left(\frac{g}{2}\right)\right], \\ V_{33} &= \mathrm{e}^{-\frac{9D}{4}}\left[\mathrm{e}^{\frac{9K}{4}}\cosh(3g) - \mathrm{e}^{-\frac{9K}{4}}\right], \\ V_{34} &= \mathrm{e}^{-\frac{5D}{4}}\left[\mathrm{e}^{-\frac{3K}{4}}\cosh\left(\frac{g}{2}\right) + \mathrm{e}^{\frac{3K}{4}}\cosh(g)\right], \\ V_{44} &= \mathrm{e}^{\frac{1}{4}(K-D)}\cosh\left(\frac{g}{2}\right) - \mathrm{e}^{-\frac{1}{4}(K+g)}. \end{aligned}$$

3 Results and Discussions

Fig. 1 shows the LCA results for the global phase diagram in the reduced temperature $t = k_B T/zJ$ as a function of reduced crystal field ($d = \Delta/zJ$) plane for $\sigma = 1$, on a cubic simple lattice ($z = 6$) in comparison with traditional Mean Field Approximation (MFA) and Monte Carlo Simulations (MC). One can see that the results from LCA are systematically below the MFA results and roughly comparable to those from MC. A first-order transition has been determined from the hysteresis curve of magnetization as function of reduced temperature for a constant d as is shown in Fig. 2 (a). The TCP was determined following the criterion used in [6] which considers the variation of the magnetization (order parameter m) as a function of d for a constant t, as depicted in Fig. 2 (b).

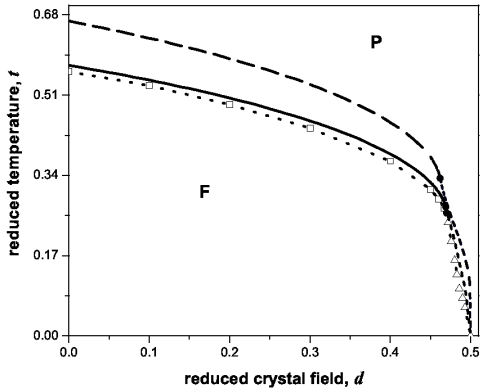

Fig. 1: Phase diagram in the $(d - t)$-plane for the generalized Ising model with $S = 1$ obtained from: MFA (long-dashed line is second-order, dashed line is first-order); LCA (solid line is second-order, short-dashed line is first-order); MC (open squares are second-order, open triangular are first-order, dot lines are guide to the eyes). The full circles represent the corresponding TCPs.

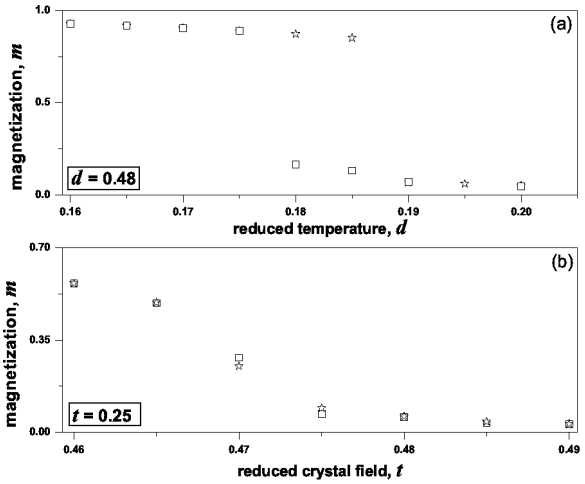

Fig. 2: Some typical results from MC simulations. (a) Magnetization as a function of t for $d = 0.48$, open squares are for increasing t and open stars for the ones decreasing. The first-order transition temperature was estimated at $t = 0.18(3)$ (b) Magnetization as a function of d for $t = 0.26$, open squares and stars have meaning the same as in (a). The tricritical temperature was estimated at $t_T = 0.26$.

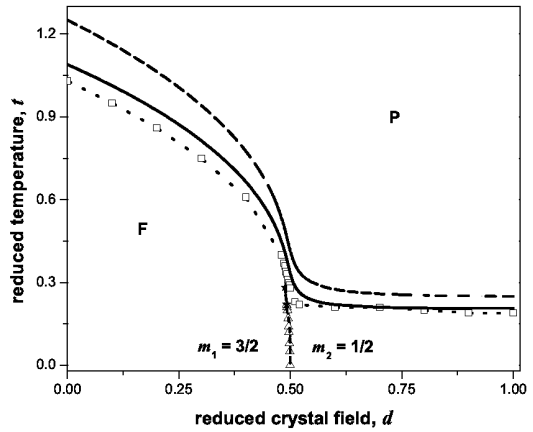

Fig. 3: The same as Fig. 1 for $\sigma = \frac{3}{2}$. In this case there is not TCP but there exists an isolated multiphase critical point denoted by $\star$.

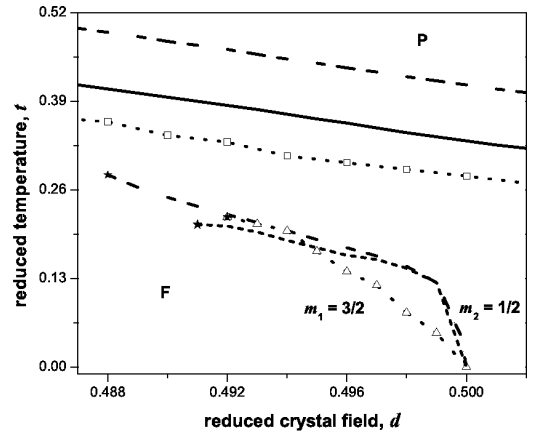

Fig. 4: Low temperature phase diagram in the $d-t$-plane. The isolated multiphase critical point is represented by $\star$. There are two different ferromagnetic phases denoted by $m_1 = \frac{3}{2}$ and $m_2 = \frac{1}{2}$ as $t \to 0$.

The global phase diagram for $\sigma = 3/2$ is shown in Fig. 3 where there is no TCP with the upper transition line being always second-order. The unique first-order transition line separating the two ordered phases ($m_1 = 3/2$ and $m_2 = 1/2$, m is the magnetization) finishes at an isolated multiphase critical point, in complete agreement with traditional MFA [3]. Fig. 4 shows, with more details, the low temperature region of the phase diagram depicted in Fig. 3. The unique first-order transition line separating the two ordered phases terminates at a multiphase critical point far from the second-order transition in contrast with predicted by [7, 8, 9]

4 Conclusions

The general spin-S Ising model has been studied using the LCA and MC simulations. Full phase diagrams have been analyzed, specially in the low temperature region, where a number of first-order lines emerge. For $\sigma = 1$ the results from the LCA in three-dimensions are qualitatively the same with Monte Carlo simulations for a cubic lattice. So, the present results for $S = \frac{3}{2}$ are contrary to the predictions from real space renormalization group approaches [7, 8], as well as previous Monte Carlo simulations [9].They are, however, in qualitative agreement with those obtained from ordinary mean field calculations [3] and an exact formulation of the model on a Cayley tree [10]. Namely, the unique first-order transition line at low temperatures does not terminate on the second-order transition line.

References

[1] M. Blume, Phys. Rev. **141**: 517 (1 966).

[2] H.W. Capel, Physica **32**: 966 (1 966).

[3] J.A. Plascak, J.G. Moreira and F.C. Sá Barreto, Phys. Lett. A **173**: 360 (1 993).

[4] H. Falk, Amer. J. Phys. **38**: 858 (1 970).

[5] H. A. Kramers and G. H. Wannier, Phys. Rev. **60**: 252 (1 941).

[6] A. K. Jan and D. P. Landau, Phys. Rev. B **22**: 445 (1 980).

[7] S. Moss de Oliveira, P. M. C. de Oliveira and F. C. Sá Barreto, J. Stat. Phys. **78**, 1 619 (1 995).

[8] A. Bakchich, A. Bassir and A. Benyoussef, Physica A **195**: 188 (1 993).

[9] F. C. Sá Barreto and O. F. de Alcântara Bonfim, Physica A **172**: 378 (1 991).

[10] M.N. Tamashiro and S.R.A. Salinas, Physica A **211**, 124 (1 994).